

KINETICS, CATALYSIS, AND REACTION ENGINEERING

ZSM-5 Coatings on Stainless Steel Grids in One-Step Benzene Hydroxylation to Phenol by N₂O: Reaction Kinetics Study**B. Louis, L. Kiwi-Minsker, P. Reuse, and A. Renken****Institute of Chemical Engineering, Swiss Federal Institute of Technology, CH-1015 Lausanne, Switzerland*

One-step hydroxylation of benzene to phenol by N₂O has been performed over structured catalytic beds made of ZSM-5 coatings on stainless steel grids. The catalysts demonstrated high activity with a selectivity toward phenol formation of 98%. A detailed kinetic study was carried out with a variation in reactant concentrations, benzene/N₂O ratio, and residence time. The results obtained suggest a surface reaction between benzene and nitrous oxide adsorbed on two different active sites.

1. Introduction

During the past decade, there has been growing interest in catalytic reactor engineering based on structured catalytic beds. Structured reactors offer several advantages compared to conventional fixed-beds and slurry reactors.^{1,2} Their open macrostructure allows for high flow rates with a low-pressure drop. The flow dynamics is better controlled, leading to improved heat and mass transfer.

Catalytic materials prepared via zeolite coatings of metal grids have recently been reported as novel structured catalysts.^{3–9} Despite the increasing interest in zeolitic coatings, only a few practical applications have been reported.^{10,11} In our previous publication ZSM-5 crystals grown on stainless steel grids were tested in the gas-phase hydroxylation of benzene by N₂O to phenol.¹² This industrially important reaction was chosen because it is exothermic and because the use of a metallic-based structured catalytic bed allows for better heat distribution. This avoids hot-spot and runaway problems. The same intrinsic reactivity, compared to traditional zeolitic fixed beds, was achieved with a 98% selectivity to phenol.¹²

The present work reports a reaction kinetics study aimed on a development of a suitable kinetic model that is useful for process optimization and scale-up.

2. Experimental Section**2.1. Catalyst Preparation and Characterization.**

The support used for the preparation of the structured zeolitic materials was stainless steel AISI 316 type supplied by Haver and Boecker (Oelde Westfalen, Germany). It contains chromium (16.5–18.5%), nickel (11–14%), molybdenum (2–2.5%), and iron (65–70%). The wire diameter and the mesh size were 250 and 800 μm, respectively. The support packing was 70 mm in length and 34 mm in width and was formed by a superposition of 15 plates (see Figure 1). Each plate (9

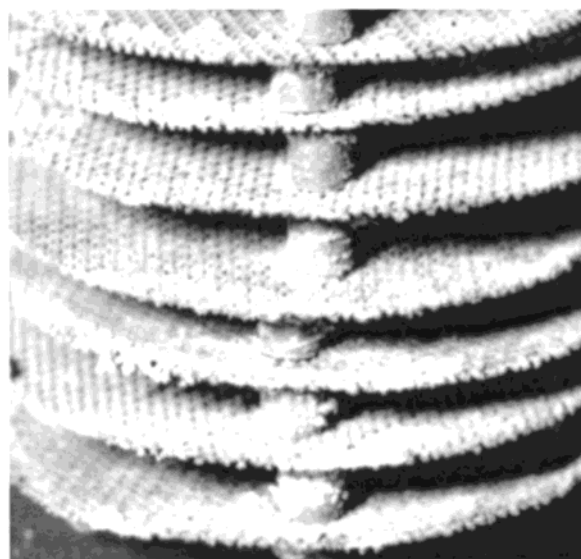


Figure 1. Structured catalytic bed made from stainless steel grids coated by HZSM-5.

cm²) was separated from the others by steel rings of 4 mm length. The whole support packing was pretreated in boiling toluene for 2 h and in a 15% hydrochloric acid solution for 20 min in order to remove organic and inorganic contaminants. Afterward, the packing was rinsed in distilled water under ultrasonic treatment. This procedure is known to create defects on the metal surface that become crystallization centers during the synthesis of the zeolite coating.^{7,8}

The mixture for the ZSM-5 synthesis was prepared by adding, at room temperature, sodium aluminate, sodium chloride, tetrapropylammonium hydroxide, and tetraethyl orthosilicate to demineralized water with the molar ratios reported previously.¹² Ageing and homogenization of the mixture were performed for 2–3 h. The gel was then poured into a 250-mL Teflon-lined autoclave containing the vertically positioned catalytic support packing. The temperature was increased within 1 h up to 444 K, and the zeolite synthesis took place for 40 h under autogenous pressure. The synthesis proce-

* To whom correspondence should be addressed. E-mail: albert.renken@epfl.ch.

ture was repeated three times with a fresh solution each time to enhance the weight of the zeolite coating. Finally, the packing was kept in an ultrasonic bath (45 kHz) for 20 min to remove loosely attached crystals and was dried overnight at 400 K. The three-step synthesis was followed by calcination overnight at 773 K in air. The MFI structure was obtained in sodium form, was exchanged three times with ammonium chloride (0.1 M) at 353 K, and was then calcined at 773 K for 5 h in air, resulting in H-ZSM5 (totally 1.45 g).

The specific surface area of the catalysts was determined by nitrogen adsorption (77 K) employing the BET method with a Sorptomatic 1900 (Carlo-Erba) instrument. X-ray diffraction (XRD) patterns of powdered catalysts were measured out on a Siemens D5000 ($\theta/2\theta$) diffractometer with Cu K α monochromatic radiation ($\lambda = 1.5406 \text{ \AA}$). The surface morphology and the thickness of the crystalline layer (zeolite coating) were studied by scanning electron microscopy on a JEOL JSM 6300F apparatus. The Si/Al ratio of the crystals was determined by energy dispersive X-ray (EDX) analysis coupled with the SEM chamber.

2.2. Experimental Setup and Procedure. The setup used for the kinetics study consists of a feed section, an analytical part, and a stainless steel tubular reactor (340 mm length and 34 mm diameter). Nitrous oxide and nitrogen (>99.95%, Carbagaz, Lausanne, Switzerland) were supplied through mass flow controllers (Bronkhorst High-Tech B. V., Ruurlo, The Netherlands). Nitrogen was used as a carrier gas and could pass through one of the two bubble columns: one column contained water used during pretreatment of the catalyst for its activation/regeneration and the other contained benzene for the reaction. The analytical part was equipped with an on-line gas chromatograph (Shimadzu GC-14A, 30m HP-5, FID) to analyze benzene and phenol. Higher hydrocarbons and polyaromatics were analyzed off-line by a GC-MS (Hewlett-Packard, HPG1800A GCD system, HP-5). CO₂ formation and the N₂O concentration were monitored with an IR analyzer (Siemens Ultramat-22P).

Measurements of the residence time distribution showed that the reactor has the characteristics of a plug-flow reactor. A four-block oven (Vinci Technologies, France) was used to heat the reactor. The temperature was measured in the middle part of the reactor by a K-type thermocouple (Phillips AG, Dietikon, Switzerland). The pressure was regulated by needle valves (Hoke 1315-4S).

The zeolite structured catalytic bed was placed into the reactor and activated at 823 K for 1 h under nitrogen flow. For the kinetic studies, the benzene to nitrous oxide (B/N) ratio was varied from 0.2 to 8.9 with a constant benzene concentration of 0.78 mol m⁻³. At a constant N₂O concentration (0.82 mol m⁻³), the B/N ratio was varied from 0.8 to 4.1. The total flow was always set to 60 STP mL/min by addition of N₂. The reaction was carried out at 623 K and atmospheric pressure.

The conversions of benzene and nitrous oxide (X_B and X_{N_2O}) were calculated from the difference between the reactor inlet and outlet concentrations of each reactant. The selectivity toward phenol was defined as the molar ratio of the phenol obtained to the benzene converted. The conversion and yield were measured after the transient period of ca. 50 min. Afterward, only a slight deactivation of the catalyst (ca. 1% per hour) occurred.

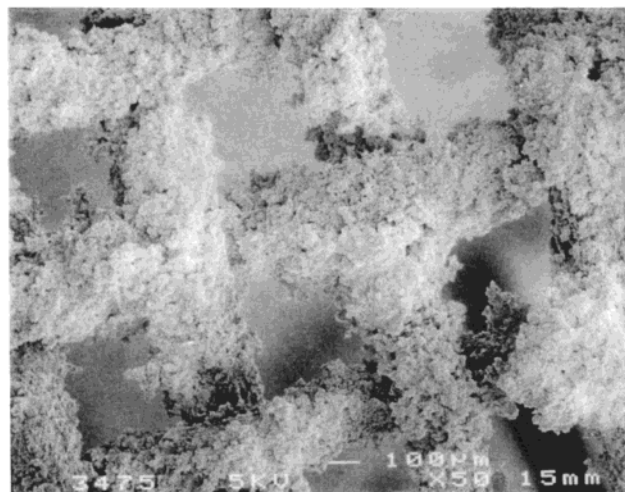


Figure 2. SEM photograph of zeolitic coatings: surface of one grid.

After 3 h on stream, the catalyst was regenerated overnight under air flow at 773 K to restore the initial activity. Because the conversions of benzene achieved were less than 15%, the rate of benzene transformation was calculated by multiplying the difference between the benzene concentrations at the reactor inlet and outlet by the total flow, referred per gram of ZSM-5 coated.

As the conversions of nitrous oxide were much higher (up to 80%), the concentration profiles along the reactor length could not be neglected. Therefore, an integral form for the equations was considered to describe the rate of N₂O transformation.

3. Results

3.1. Catalyst Characterization. A total coverage of 95 g of ZSM-5/m² of grid was obtained after the three-step coating procedure. Figure 2 represents a SEM micrograph of the surface of the structured zeolitic coating showing that no part of the metal support remains uncovered. The thickness of the zeolite layer was estimated to be about 40 μm . Further coating was found not to be reasonable for the grid geometry used in this study because the void fraction decreased drastically, leading to a high pressure drop during the passage of gas through the catalytic bed. The elemental analysis of the zeolitic layer studied by EDX analysis found a Si/Al ratio of 65. The iron content, as measured by atomic absorption spectroscopy, was found to be less than 0.1 wt %.

The XRD powder pattern confirmed the MFI structure.¹² The BET surface area was 302 m²/g of ZSM-5 with a total pore volume of 0.29 cm³/g of ZSM-5.

3.2. Activity/Selectivity of ZSM5 Coatings in Benzene Hydroxylation. The rate of reaction has been estimated to be about 10⁻⁷ mol of benzene consumed per gram of ZSM-5 per second. This value corresponds to those obtained by other authors with the granulated form of ZSM-5,^{13,14} confirming the lack of any effect of the metal on the intrinsic catalytic performance.

Mass transfer is known to limit many reactions catalyzed by zeolites. On the basis of the criteria of Mears¹⁵ and considering $R_V = 0.04 \text{ mol m}^{-3} \text{ s}^{-1}$ (rate of reaction referred to the catalyst volume), $Re = 10^{-2}$, and

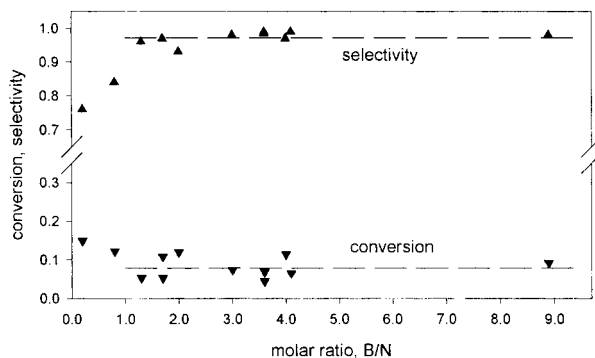


Figure 3. Conversion and selectivity to phenol as a function of the B/N ratio.

$Sc = 1$, it was found that any external mass transfer limitation can be excluded ($Da_{II} = 10^{-4}$).

The diffusion coefficient for benzene in ZSM5 is estimated to be on the order of $D_B = 10^{-13} \text{ m}^2/\text{s}$ (Kärger and Ruthven¹⁶). With a crystal size of $d_p = 1 \mu\text{m}$, a Weisz module in the range of $0.1 < \phi < 0.2$ results. As the catalyst efficiency is found to be higher than 90% for $\phi < 0.3$,¹⁵ the influence of internal mass transfer on the observed reaction rate can be neglected.

As already reported in the literature, a high selectivity at appreciable conversions can be achieved with H-MFI type zeolites.^{17–21} The main product formed in our experiments was phenol, with a selectivity of up to 98%. Carbon dioxide was the major byproduct observed, whereas quinones and biphenyl were found in trace concentrations. By control experiments, it was verified that the stainless steel support alone did not catalyze any transformations of benzene and N_2O at the reaction temperature used.

Figure 3 shows the evolution of the conversion and selectivity with different benzene/nitrous oxide (B/N) ratios. An excess of nitrous oxide is known to be beneficial for benzene conversion for traditional fixed beds.^{22,23} For $B/N < 1$ and $C_{\text{N}_2\text{O}} > 1 \text{ mol/m}^3$, a decrease in the benzene-to-oxidant ratio leads to a loss in selectivity toward phenol in favor of carbon dioxide. This indicates that the total oxidation route is strongly dependent on the concentration of nitrous oxide, whereas the phenol formation is only slightly influenced by its concentration. The further oxidation products such as quinones are formed in a consecutive step.¹⁷ Reducing the concentration of nitrous oxide to 0.1 mol m^{-3} suppresses benzoquinone formation, which has been detected in traces for the ratio $B/N = 8.9$. An increase in selectivity toward phenol from 76 to 99% was observed with an increase in benzene concentration,¹² in agreement with the results reported by Kustov et al.²⁴ An improvement in phenol selectivity at high benzene-to-nitrous oxide ratios was explained by adsorption effects.²⁵ Emig et al.¹⁷ assumed that an excess of benzene could displace the adsorption–desorption equilibrium between benzene and phenol. Thus, phenol desorption would be facilitated, reducing its surface concentration and the occurrence of consecutive reactions.

3.3. Kinetic Model. There is general agreement in recent literature that the reaction proceeds via the decomposition of N_2O into an active form of oxygen, probably on a Lewis site, the nature of which is still under debate.^{19–21,23,24,26–28}

There is no formal evidence for benzene adsorption. However, Haw demonstrated by H/D exchange experi-

ments and theoretical investigations that an interaction between benzene and the zeolite framework occurs.^{29–31} These results are also supported by diffraction studies of the $\text{C}_6\text{D}_6/\text{MFI}$ system.³² Therefore, an intermediate “benzenium” species could be formed on Brönsted acid sites.²⁹

The following kinetic model was developed by considering adsorption of nitrous oxide and benzene on two distinct sites:

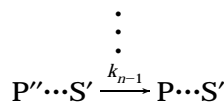
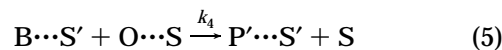
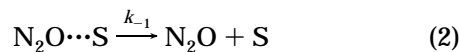
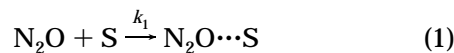


Figure 3 shows that the selectivity toward phenol remains close to 100% for benzene-to- N_2O ratios higher than 1. Thus, we consider that the totality of benzene and nitrous oxide were consumed to produce phenol.

To estimate the model parameters, two different reaction conditions were chosen.

Constant C_B and Variation of $C_{\text{N}_2\text{O}}$. The benzene concentration at the reactor inlet was kept constant (0.78 mol m^{-3}), while the N_2O concentration was varied from 0.1 to 3.4 mol m^{-3} .

Langmuir adsorption for nitrous oxide on site S (eqs 1 and 2) and decomposition of N_2O to nitrogen and an active oxygen species (eq 3) are assumed. Under steady-state conditions, the surface concentrations of nitrous oxide and the active oxygen species are given by the following relationships:

$$\Theta_{\text{N}_2\text{O}} = \frac{K_{\text{N}_2\text{O}} C_{\text{N}_2\text{O}}}{1 + K_{\text{N}_2\text{O}} \left(1 + \frac{k_2}{k_4}\right) C_{\text{N}_2\text{O}}} \quad (7)$$

with

$$K_{\text{N}_2\text{O}} = k_1/(k_{-1} + k_2)$$

$$\Theta_{\text{O}} = \frac{k_2}{k_4} \Theta_{\text{N}_2\text{O}} \quad (8)$$

The parameter k_4 includes the (constant) surface concentration of benzene.

The rate of N_2O transformation is therefore

$$-R_{N_2O} = \frac{K'K''_{N_2O}C_{N_2O,0}(1-X)}{1 + K''_{N_2O}\left(1 + \frac{k_2}{k_4}\right)C_{N_2O,0}(1-X)} = C_{N_2O,0} \frac{dX}{d\tau} \quad (9)$$

$$\frac{dX}{d\tau} = \frac{K'K''_{N_2O}(1-X)}{1 + K''_{N_2O}C_{N_2O,0}(1-X)} \quad (10)$$

with

$$K''_{N_2O} = K''_{N_2O} \left(1 + \frac{k_2}{k_4}\right)$$

where $C_{N_2O,0}$ corresponds to the initial concentration of N_2O , X designates the N_2O conversion, τ is the space time, and K' is a global rate constant that includes the average benzene concentration in the gas. An integral form of the kinetic equations was used to describe the nitrous oxide transformation.

Integration of eq 10 leads to

$$C_{N_2O,0}X = \frac{K'K''_{N_2O}}{K''_{N_2O}}\tau + \frac{1}{K''_{N_2O}} \ln(1-X) = K''\tau + \frac{1}{K''_{N_2O}} \ln(1-X) \quad (11)$$

Figure 4 shows the linear dependence of the N_2O concentration as a function of the logarithm of $(1-X)$. This indicates that the proposed model can be applied to describe the experimental data correctly. The parameter K''_{N_2O} corresponds to an apparent equilibrium constant. Its value was $67 \text{ m}^3/\text{mol}$, and it was used to estimate the surface coverage of N_2O .

Figure 5 represents the calculated coverage of sites S by nitrous oxide as a function of its gas-phase concentration. For $C_{N_2O} > 0.1 \text{ mol/m}^3$, a nearly complete coverage is obtained ($\theta_{N_2O} > 0.9$). Therefore, the nitrous oxide concentration in the gas phase has no significant influence on the reaction rate, and a zero-order dependence on N_2O is observed. This is in line with the results reported by Suzuki et al.²² on dumped packed-bed reactors.

Constant C_{N_2O} and Variation of C_B . Experiments at two different inlet concentrations of N_2O (0.41 and 0.82 mol m^{-3}) were performed, with the benzene concentration varying from 0.5 to 3.4 mol m^{-3} . In this concentration range, a zero-order dependence on nitrous oxide ($C_{N_2O} > 0.1 \text{ mol m}^{-3}$ at the reactor outlet and $B/N > 1$) was observed.

Figure 6 shows the rate of benzene transformation as a function of its average concentration in the reactor (difference between inlet and outlet concentrations). Three series of experiments were carried out with the same time of contact, showing an increase in the reaction rate with benzene concentration. It can clearly be seen that the order of reaction toward benzene is between 0 and 1, indicating a multistep process.

The MFI structure is known to possess a strong electrostatic field. On the basis of general considerations of confinement theory and phenols higher polarity and larger size, phenol should be more strongly adsorbed on the catalyst surface than benzene.^{33,34}

To examine the validity of this statement, the zeolite was dissolved after reaction in a hydrofluoric acid solution (40%). Then the soluble components were

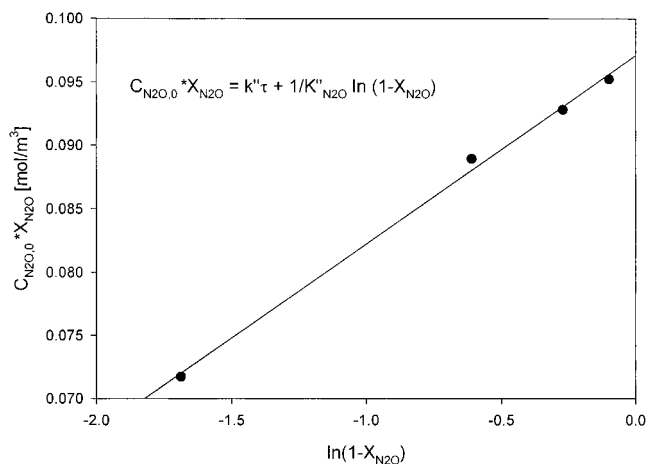


Figure 4. Dependence of the rate of N_2O consumption on the logarithm of $(1-X)$.

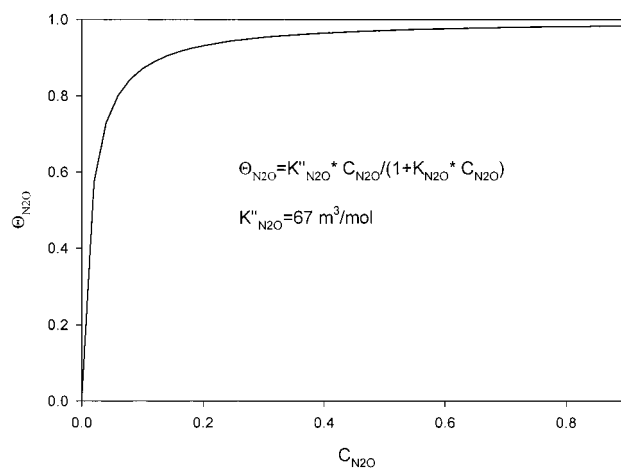


Figure 5. Langmuir model: coverage dependence on the gas-phase N_2O concentration.

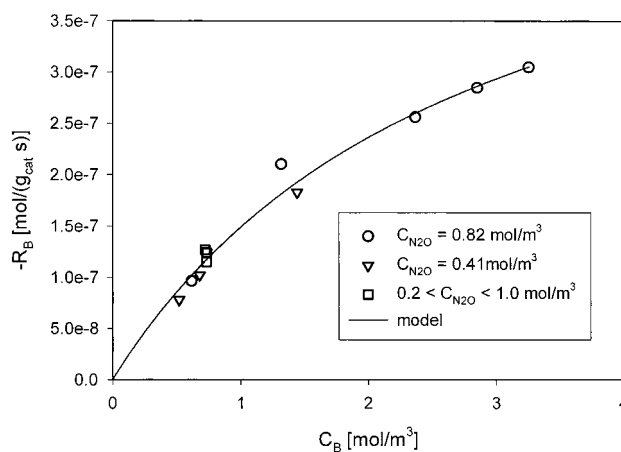


Figure 6. Rate of benzene consumption as a function of the average benzene concentration in the reactor, $C_B = (C_B^{\text{in}} - C_B^{\text{out}})/2$.

extracted with a solvent, as already reported by Magnoux.³⁵ Only phenol was detected by GC and GC-MS.

Therefore, the MASI (most abundant surface intermediate) model considering a predominantly adsorbed species on the surface³⁶ was used to describe the experimental results. After the adsorption of benzene on a vacant site S' (eq 4), followed by $(n-1)$ unspecified steps, the MASI-P... S' - (adsorbed phenol) is formed. All of these $(n-1)$ steps are supposed to proceed faster than desorption; thus, the adsorbed phenol is considered

to be the most abundant intermediate on the catalyst surface. Phenol desorbs (eq 6), restoring a free site S' on which benzene can be adsorbed.

Under steady-state conditions

$$R = R_3 = R_{n-1} = R_n \quad (12)$$

$$-R_B = k_3(1 - \Theta'_p) = k_n\Theta'_p \quad (13)$$

where Θ'_p represents the fraction of sites S' covered by phenol and $(1 - \Theta'_p)$ corresponds to the fraction of free sites. Resolution of eq 13 leads to the expression for the surface coverage by phenol

$$\Theta'_p = \frac{k_3 C_B}{k_n + k_3 C_B} = \frac{K'_B C_B}{1 + K'_B C_B} \quad (14)$$

with $K'_B = k_3/k_n$, which corresponds to the ratio of the adsorption rate constant for benzene to the desorption rate constant for phenol.

Combining eq 13 and 14 leads to the expression for the rate of benzene transformation.

$$-R_B = \frac{k_3 C_B}{1 + \frac{k_3}{k_n} C_B} \quad (15)$$

The model parameters of eq 15 were estimated by fitting them to the experimental data, and the results are shown on Figure 6 with the following parameters found: $k_3 = 2.3 \times 10^{-7} \text{ m}^3 \text{ g}^{-1} \text{ s}^{-1}$ and $k_n = 5.2 \times 10^{-7} \text{ mol g}^{-1} \text{ s}^{-1}$.

Figure 3 shows a decrease in selectivity in favor of carbon dioxide at N_2O concentrations higher than 1 mol m^{-3} ($\text{B/N} < 1$). To explain this experimental observation, we have to assume a parallel pathway of a nonselective total oxidation of adsorbed phenol (or another intermediate) by nitrous oxide from the gas phase.



Thus, when the N_2O concentration is higher than 1 mol m^{-3} , this pathway decreases the selectivity to phenol and increases the total reaction rate through a supplementary liberation of the active sites of type S' .

4. Conclusions

ZSM-5 coatings on stainless steel grids have proven to be effective catalysts for the one-step production of phenol via benzene hydroxylation by nitrous oxide.

The kinetic results obtained suggest a Langmuir–Hinshelwood mechanism in which benzene and nitrous oxide are adsorbed on two distinct active sites.

The nitrous oxide concentration obeys a Langmuir isotherm. For the concentration of nitrous oxide $C_{\text{N}_2\text{O}} > 0.1 \text{ mol/m}^3$, the surface coverage is close to 100%, and a zero-order dependence on N_2O is observed.

The MASI model describes well the experimental dependences between the reaction rate and the concentration of benzene.

At molar ratios of $\text{B/N} > 1$, the selectivity toward phenol formation was 98%. Therefore, low concentra-

tions of oxidant should be used to reduce cost, separation problems, and environmental impacts.

Acknowledgment

The authors gratefully acknowledge financial support from the Swiss National Science Foundation and M. P. Möckli, E. Casali, and B. Senior (EPFL) for technical assistance in catalyst characterization.

Notation

C = concentration (mol/m^3)
 Da_{II} = second number of Damköhler
 k = kinetic constant
 K_N = apparent equilibrium constant of nitrous oxide adsorption
 P = phenol
 R = rate of reaction
 Re = Reynolds number
 S = site for N_2O adsorption
 S' = site for benzene adsorption
 Sc = Schmidt number
 X = conversion

Greek Letters

θ = fraction of surface covered
 τ = space time
 ϕ = Weisz module

Subscripts

1 = adsorption step
 B = benzene
 n = desorption step
 N = nitrous oxide
 P = phenol
 t = total oxidation
 V = volume

Literature Cited

- (1) Cybulski, A.; Moulijn, J. A. *The present and the future of structured catalysts—An overview. Structured catalysts and reactors*; Marcel Dekker: New York, 1998.
- (2) Kiwi-Minsker, L.; Yuranov, I.; Höller, V.; Renken, A. Supported glass fiber catalysts for novel multiphase reactor design. *Chem. Eng. Sci.* **1999**, *54*, 4785.
- (3) Jansen, J. C.; Nugroho, W.; van Bekkum, H. Controlled growth of thin films of molecular sieves on various supports. *Proceedings of the 9th International Zeolite Conference*, July 5–10, 1992, Montreal, Canada; von Ballmoos, R., Higgins, J.B., Treacy, M. M. J., Eds.; Butterworth–Heinemann: Boston, MA, 1993.
- (4) Calis, H. P.; Gerritsen, A. W.; van den Bleek, C. M.; Legein, C. H.; Jansen, J. C.; van Bekkum, H. Zeolites grown on wire gauze: A new structured catalyst packing for dustproof, low-pressure drop DeNox processes. *Can. J. Chem. Eng.* **1995**, *73*, 120.
- (5) Jansen, J. C.; Kashchiev, D.; Erdem-Senatalar, A. Preparation of coatings of molecular sieve crystals for catalysis and separation. *Stud. Surf. Sci. Catal.* **1994**, *85*, 215.
- (6) Shan, Z.; van Kooten, W. E. J.; Oudshoorn, O. L.; Jansen, J. C.; van Bekkum, H.; van den Bleek, C. M.; Calis, H. P. A. Optimization of the preparation of binderless ZSM-5 coatings on stainless steel monoliths by in situ hydrothermal synthesis. *Microporous Mater.* **2000**, *34*, 81.
- (7) Valtchev, V.; Mintova, S. The effect of the metal substrate composition on the crystallization of zeolite coatings. *Zeolites* **1995**, *15*, 171.
- (8) Mintova, S.; Valtchev, V.; Konstantinov, L. Adhesivity of molecular sieve films on metal substrates. *Zeolites* **1996**, *17*, 462.
- (9) Yan, Y.; Bein, T. Zeolite thin films with tunable molecular sieve function. *J. Am. Chem. Soc.* **1995**, *117*, 9990.
- (10) Jansen, J. C.; Koegler, J. H.; van Bekkum, H.; Calis, H. P. A.; van den Bleek, C. M.; Kapteijn, F.; Moulijn, J. A.; Geus, E.

R.; van der Puil, N. Zeolitic coatings and their potential use in catalysis. *Microporous Mater.* **1998**, *21*, 213.

(11) van Bekkum, H.; Geus, E. R.; Kouwenhoven, H. W. Supported zeolite systems and applications. *Stud. Surf. Sci. Catal.* **1994**, *85*, 509.

(12) Louis, B.; Reuse, P.; Kiwi-Minsker, L.; Renken, A. Synthesis of ZSM-5 coatings on stainless steel grids and their catalytic activity for partial oxidation of benzene by N_2O . *Appl. Catal.* **2001**, *210*, 103.

(13) Uriarte, A. K.; Rodkin, A. R.; Gross, M. J.; Kharitonov, A. S.; Panov, G. I. Direct hydroxylation of benzene to phenol by nitrous oxide. *Proceedings of the 3rd World Congress on Oxidation Catalysis*, Sep 21–26, 1997, San Diego, CA; Elsevier: New York, 1997; p 857.

(14) Sobolev, V. I.; Panov, G. I.; Kharitonov, A. S.; Romannikov, V. N.; Volodin, A. M.; Ione, K. G. Catalytic properties of ZSM-5 zeolites in N_2O decomposition: The role of iron. *J. Catal.* **1993**, *139*, 435.

(15) Baerns, M.; Hofmann, H.; Renken, A. *Chemische Reaktionen Technik*, 3rd ed.; Georg Thieme Verlag: Stuttgart, Germany, 1999.

(16) Kärger, J.; Ruthven, D. M. *Diffusion in zeolites and other microporous solids*; J. Wiley and Sons: New York, 1992.

(17) Häfele, M.; Reitzmann, A.; Roppelt, D.; Emig, G. Hydroxylation of benzene with nitrous oxide on H–Ga–ZSM5 zeolite. *Appl. Catal.* **1997**, *150*, 153.

(18) Gubelmann, M.; Tirel, P. J. (Rhone-Poulenc Chimie France). Preparation of phenol by direct hydroxylation of benzene. U.S. Patent 5,001,280, 1991.

(19) Motz, J. L.; Heinichen, H.; Hölderich, W. F. Direct hydroxylation of aromatics to their corresponding phenols catalysed by H–[Al]ZSM-5 zeolite. *J. Mol. Catal. A* **1998**, *136*, 175.

(20) Panov, G. I.; Sobolev, V. I.; Dubkov, K. A.; Kharitonov, A. S. Biometric oxidation on Fe complexes in zeolites. *Proceedings of the 11th International Congress on Catalysis, 40th anniversary*, June 30–July 5, 1996, Baltimore, MD; Hightower, J. W., Delgass, W. N., Iglesia, E., Bell, A. T., Eds.; Elsevier Science: New York, 1996; Vol. 101, p 493.

(21) Zholobenko, V. Preparation of phenol over dehydroxylated HZSM-5 zeolites. *Mendeleev Commun.* **1993**, 28.

(22) Suzuki, E.; Nakashiro, K.; Ono, Y. Hydroxylation of benzene with dinitrogen monoxide over H–ZSM-5 zeolite. *Chem. Lett.* **1988**, 953.

(23) Panov, G. I.; Kharitonov, A. S.; Sobolev, V. I. Oxidative hydroxylation using dinitrogen monoxide: a possible route for organic synthesis over zeolites. *Appl. Catal. A* **1993**, *98*, 1.

(24) Kustov, L. M.; Bogdan, V. I.; Kazansky, V. B. (General Electric Company). Preparation of phenol and its derivatives. European Patent 0889018, 1999.

(25) Kijenski, J.; Baiker, A. Acidic sites on catalyst surfaces and their determination. *Catal. Today* **1989**, *5*, 1.

(26) Motz, J. L.; Heinichen, H.; Hölderich, W. F. Influence of extra-framework alumina in H–[Al]ZSM-5 zeolite on the direct hydroxylation of benzene to phenol. *Stud. Surf. Sci. Catal.* **1997**, *105*, 1053.

(27) Hölderich, W. F. "One-pot" reactions: A contribution to environmental protection. *Appl. Catal.* **2000**, *194–195*, 487.

(28) Ribera, A.; Arends, I. W. C. E.; de Vries, S.; Pérez-Ramírez, J.; Sheldon, R. A. Preparation, characterization, and performance of FeZSM-5 for the selective oxidation of benzene to phenol with N_2O . *J. Catal.* **2000**, *195*, 287.

(29) Beck, L. W.; Xu, T.; Nicholas, J. B.; Haw, J. F. Kinetic, NMR and DFT study of benzene H/D exchange in zeolites: The most simple aromatic substitution. *J. Am. Chem. Soc.* **1995**, *117*, 11594.

(30) Haw, J. F.; Nicholas, J. B.; Xu, T.; Beck, L. W.; Ferguson, D. B. Physical organic chemistry of solid acids: Lessons from in situ NMR and theoretical chemistry. *Acc. Chem. Res.* **1996**, *29*, 259.

(31) White, J. L.; Beck, L. W.; Haw, J. F. Characterization of H-bonding in zeolites by proton solid-state NMR spectroscopy. *J. Am. Chem. Soc.* **1992**, *114*, 6182.

(32) Taylor, J. C. Locations of C_6D_6 molecules in the synthetic zeolite ZSM-5 at 77 K by powder neutron diffraction. *Zeolites* **1987**, *7*, 311.

(33) Derouane, E. Zeolites as solid solvents. *J. Mol. Catal.* **1998**, *134*, 29.

(34) Corma, A. Inorganic solid acids and their use in acid-catalyzed hydrocarbon reactions. *Chem. Rev.* **1995**, *95*, 559.

(35) Magnoux, P.; Roger, P.; Canaff, C.; Fouche, V.; Gnep, N. S.; Guisnet, M. New technique for the characterization of carbonaceous compounds responsible for zeolite deactivation. *Stud. Surf. Sci. Catal.* **1987**, *34*, 317.

(36) Boudart, M.; Djéga-Mariadassou, G. *Kinetics of Heterogeneous Catalytic Reactions*; Princeton University Press: Princeton, NJ, 1984.

Received for review August 11, 2000

Accepted January 10, 2001

IE000744L